Dalton Transactions

Tris(carbene)borates; alternatives to cyclopentadienyls in organolanthanide chemistry

Journal:	*Dalton Transactions*
Manuscript ID	DT-COM-03-2023-000718.R1
Article Type:	Communication
Date Submitted by the Author:	05-Apr-2023
Complete List of Authors:	Price, Amy; University of California Berkeley, Chemistry; Lawrence Berkeley Laboratory, Chemical Sciences Gupta, Ankur; Lawrence Berkeley National Laboratory, Computational Research Division de Jong, Wibe; Lawrence Berkeley National Laboratory, Computational Research Division Arnold, Polly; University of California Berkeley, Chemistry; Lawrence Berkeley Laboratory, Chemical Sciences

Tris(carbene)borates; alternatives to cyclopentadienyls in organolanthanide chemistry

Received 00th January 20xx,
Accepted 00th January 20xx

DOI: 10.1039/x0xx00000x

Amy N. Price,[a,b] Ankur Gupta,[c] Wibe de Jong,[c] Polly Arnold[a,b]*

The chemistry of the tris-carbene anion phenyltris(3-alkyl-imidazoline-2-yliden-1-yl)borate, **[C3^{Me}]$^-$** ligand, is initiated in the f-block. Neutral molecular complexes of the form **Ln(C3)$_2$I** are formed for cerium(III), while a separated ion pair **[Ln(C3)$_2$]I** forms for ytterbium(III). DFT/QTAIM computational analysis of the complexes and related tridentate tris(pyrazolyl)borate (**Tp**) supported analogs demonstrates the anticipated strength of the σ donation and confirms greater covalency in the metal-carbon bonds of the **[C3^{Me}]$^-$** complexes in comparison with those in the **Tp^{Me,Me}** complexes. The DFT calculations demonstrate the crucial role of THF solvent in accurately reproducing the contrasting molecule and ion-pair geometries observed experimentally for the Ce and Yb complexes.

Introduction

There are still relatively few ligands in f-block chemistry organometallic chemistry that bind to the f-block metal cations using only carbon atoms, despite the field now being more than fifty years old. Cyclopentadienyl ligands, monoanionic, six-electron donors $[C_5H_nR_{5-n}]^-$ (n = 1-5) have dominated the field,[1] with the cyclic dianionic ligand cyclooctadienide (COT^{2-}) close behind,[2-6] but few other competitors, e.g. cyclobutadienide, cyclononatetraenide.[7-13] Lanthanide organometallic complexes have demonstrated exciting properties, from single-molecule magnetism[14-17] and molecular qubit behavior [18,19, 20] to reductive activation of small molecules[21, 22] and photocatalytic properties.[23, 24] New robust, monoanionic, and sterically bulky alternatives to these cyclic ligand sets should further expand the capabilities of molecular f-block compounds.

N-heterocyclic carbenes (NHCs) have seen application as σ-donating ligands to metals across the periodic table, and are highly tunable.[25-29] Yet ligands which coordinate through multiple carbenes have only rarely been used to bind f-block cations.[30-34] We recently reported, in collaboration with the Jenkins group, the use of macrocyclic tetradentate, dianionic tetracarbenes **[^{BMe2,Me}TC^{H}]$^-$** in Fig. 1, to form homoleptic thorium (IV) and uranium (IV) carbene 'sandwich' complexes.[35]

Neutral, homoleptic bis(NHC)borate complexes have been made for a few rare earth trications (Y, Tb, Dy, Ho, Er), and the ligand field that they imparted on the Tb and Dy ions shown to generate single-molecule magnet (SMM) behavior with a magnetization relaxation that is orders of magnitude slower than in the isomeric bis(pyrazolyl)borate analogues.[36]

We considered that the monoanionic, phenyltris(3-alkyl-imidazoline-2-yliden-1-yl)borate **[C3^{R}]$^-$** in Fig. 1, which has been used extensively to support first-row transition metal complexes with unusual electronic structures, [37-41] could

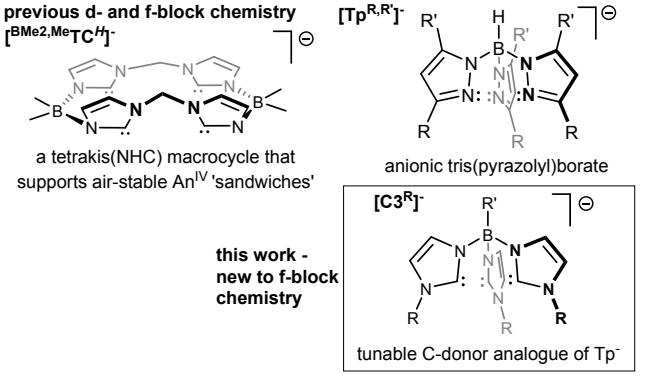

Figure 1. Multidentate ligands with anionic borate backbones as potential replacements for carbocyclic anions such as cyclopentadienyl, Cp^-.

support unusual new f-block chemistry.[42] It is isolobal to Cp^- and the tris(pyrazolyl)borate ligand **[Tp$^{R,R'}$]$^-$** in Fig. 1, an N_3-donor that has a long history in f-block chemistry.[43, 44] The **C3** ligand is readily tunable with a range of substituents reported including R = Me, Et, tBu and mesityl, and R' = H, Ph.[45-48] The triscarbene **C3^{Me}** is similar in size to the Tp* ligand (R, R' = Me), which has been used in preparing bis-Tp* lanthanide complexes. However, the Tp* ligand has been shown to be prone to BN cleavage,[44, 49, 50] which is not reported for the **C3** ligand.

Here, we report **C3** complexes of Ce^{III} and Yb^{III}, representing the beginning and end of the series, and a DFT/QTAIM computational analysis of their electronic structures, which is compared with those of their Tp* analogues. Topological analyses of the metal complexes using the QTAIM[51] theory have helped us further understand and quantify the covalent nature of the metal-ligand bonds. The QTAIM metrics, the ratio of Lagrangian kinetic energy and potential energy density at the bond critical point (BCP) (commonly represented as $\frac{-G_{BCP}}{V_{BCP}}$ symbolically) and the delocalization index ($\delta(\mathbf{M},\mathbf{X})$) have been found to be effective in identifying covalency trends in actinide complexes.[52, 53] Therefore, we have applied these metrics in the present work to broaden their applicability.

Results and Discussion

[a] Chemical Sciences Division, Lawrence Berkeley National Laboratory Berkeley, CA 94720, USA
[b] Department of Chemistry, University of California, Berkeley Berkeley, CA 94720-1460, USA.
[c] Computer Sciences Division, Lawrence Berkeley National Laboratory Berkeley, CA 94720, USA

Electronic Supplementary Information (ESI) available: [Additional information about synthesis, crystallography and calculations, Crystal structure cifs deposited in the CSD (2235950-2235953)]. See DOI: 10.1039/x0xx00000x

The cerium complex **Ce(C3)$_2$I** can be obtained from the reaction of two equivalents of **Li[C3]** and $CeI_3(thf)_4$ at room temperature, Scheme 1. **Ce(C3)$_2$I** was found to be stable in thf at 70°C for up to 80 hours with only minor degradation, while the tris(pyrazolyl)borate analog **Ce(Tp*)$_2$I** was reported to be unisolable due to B-N cleavage,[49] although it could be made *in situ* and converted to the stable bipyridyl adduct **Ce(Tp*)$_2$(bipy)**, which contains a formally mono-reduced bipy·$^-$ radical anion. To enable comparisons of the chelate ligands, we made **Ce(C3)$_2$(bipy)** from the reaction between **Ce(C3)$_2$I** and K[bipy] in THF.

Ytterbium(III) is significantly smaller than Ce(III) ($r_{cov,\ 6\text{-coord}}$ Ce^{III} = 1.15; Yb^{III} = 1.008 Å)[54]. The reaction of $YbI_3(thf)_{1.5}$ with two equivalents of **Li[C3]** results in the formation of a separated ion pair **[Yb(C3)$_2$]I**, with two [**C3**]$^-$ ligands coordinated to the ytterbium center, and an outer-sphere iodide. This is analogous to the separated ion pair [Yb(Tp*)$_2$]OTf.[55]

Once made, **[Yb(C3)$_2$]I** is insoluble in THF, unlike molecular **Ce(C3)$_2$I** which is highly THF-soluble. An attempt to prepare **Yb(C3)$_2$** from ytterbium diiodide and two equivalents of **Li[C3]** instead led to the isolation of crystals of **[Yb(C3)$_2$]I**, alongside the deposition of a grey material presumed to be ytterbium metal, suggesting a preference of the **C3** ligand for higher oxidation state metal complexes. This is in contrast to the Tp* analogue, for which the Yb(II) complex is reported to be readily isolable.[55]

The mono(**C3**) complex **Li(thf)$_4$[Ce(C3)I$_3$]** can also be made from the equimolar reaction between $CeI_3(thf)_4$ and **Li[C3]** (see SI for details and the solid state structure). Addition of a second equivalent of **Li[C3]** to **Li(thf)$_4$[Ce(C3)I$_3$]** swiftly gives **Ce(C3)$_2$I**, observed via ^{1}H-NMR spectroscopy, although addition of further $CeI_3(thf)_4$, quickly regenerates **Li(thf)$_4$[Ce(C3)I$_3$]**, Scheme 1, demonstrating that the [**C3**] NHC chelate binds Ce^{III} more strongly than Li^I but that these monoanions can exchange rapidly. The solid-state structures of the three bis(**C3**) complexes (Figure 1) are discussed below along with the computation results arising from DFT geometry optimizations and electronic structure calculations (Table 1 above, further details are included in the SI).

The structures of **Ce(C3)$_2$I** and **Ce(C3)$_2$(bipy)** are similar, with a B-Ce-B angle of 144.64(5)° in **Ce(C3)$_2$I** and 144.64(5)° in

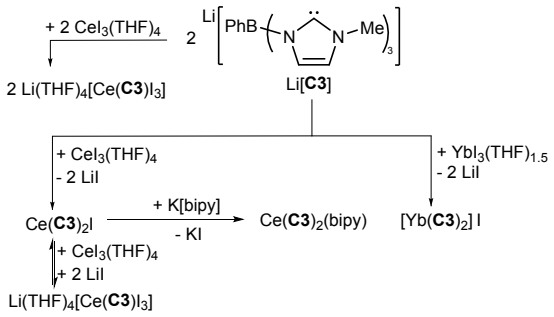

Scheme 1: Ce and Yb complexes of [**C3**]$^-$ can be prepared from Li[**C3**]$^-$ and the respective $LnI_3(thf)_n$ salt via salt metathesis. All reactions were conducted in thf at room temperature.

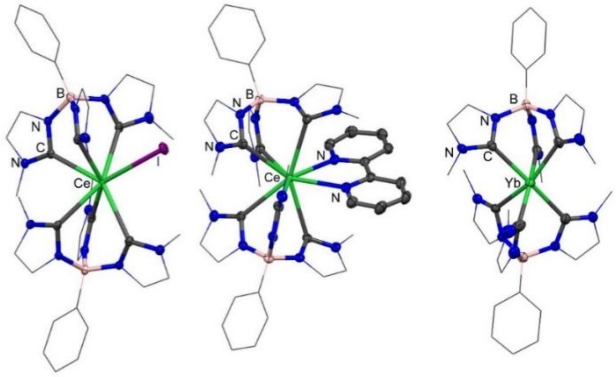

Figure 2. Solid-state structures of a) **Ce(C3)$_2$I**, b) **Ce(C3)$_2$(bipy)**, and c) the cation of **[Yb(C3)$_2$]I**. peripheral carbons drawn as wireframe, hydrogen atoms, lattice solvent, and iodide counterion in c) omitted for clarity. C= grey, Ce, Yb= green, N=blue B=pink, I=purple.

Table 1. QTAIM metrics for the metal-ligand bonds in the optimized lanthanide borate complexes. **BCP** = Bond critical point, $\boldsymbol{\rho_{BCP}}$ = Electron density at BCP, $\boldsymbol{\nabla^2\rho_{BCP}}$ = Laplacian of the electron density at BCP, $\boldsymbol{G_{BCP}}$ = Lagrangian kinetic energy, $\boldsymbol{V_{BCP}}$ = Potential energy density, $\boldsymbol{\delta(M,X)}$ = Delocalization Index

Metal Complex	Bond Length (Å)	$\boldsymbol{\rho_{BCP}}$	$\boldsymbol{\nabla^2\rho_{BCP}}$	$\boldsymbol{\frac{-G_{BCP}}{V_{BCP}}}$ (Mean)	$\boldsymbol{\delta(M,X)}$ (Mean)
Ce(C3)$_2$I	2.63 – 2.84	0.034 – 0.053	0.063 – 0.083	0.767 – 0.855 (0.801)	0.253 – 0.346 (0.306)
[Yb(C3)2]I	2.43 – 2.50	0.052 – 0.060	0.122 – 0.142	0.803 – 0.820 (0.811)	0.288 – 0.326 (0.304)
Ce(C3)$_2$ (bipy)	2.70 – 2.82	0.032 – 0.045	0.062 – 0.080	0.810 – 0.873 (0.832)	0.216 – 0.302 (0.270)
Ce(Tp*)$_2$ (bipy)	2.57 – 2.71	0.036 – 0.049	0.095 – 0.124	0.864 – 0.921 (0.893)	0.212 – 0.275 (0.239)
[Yb(Tp*)$_2$]I	2.31 – 2.35	0.061 – 0.066	0.201 – 0.216	0.854 – 0.866 (0.861)	0.287 – 0.314 (0.296)

Ce(C3)$_2$bipy. The Ce-C range is 2.631(2) - 2.781(2) Å in **Ce(C3)$_2$I**, slightly shorter than in **Ce(C3)$_2$(bipy)** (2.7016(17) to 2.8270(17) Å), likely due to reduced steric hindrance about cerium in the former. (Median Ce(III) carbene distance in CCDC = 2.749 Å.) The computed Ce-C bonds agree with experiment, and are in line with greater covalency of the Ce-C bonds in **Ce(C3)$_2$I**.

The $\boldsymbol{\frac{-G_{BCP}}{V_{BCP}}}$ ratio is typically between 0.5 and 1.0 for covalent bonds, with a lower value indicating a higher degree of covalency; while $\boldsymbol{\delta(M,X)}$ represents the approximate number of electron pairs shared between two atomic basins; a higher $\boldsymbol{\delta(M,X)}$ value for a bond signifies a higher level of covalency. Calculated values of $\boldsymbol{\rho_{BCP}}$ and $\boldsymbol{\nabla^2\rho_{BCP}}$ for the Ce-C bonds indicate that the Ce-C bonding is primarily ionic, while $\boldsymbol{\frac{-G_{BCP}}{V_{BCP}}}$ is calculated to range between 0.767-0.855 for **Ce(C3)$_2$I** and 0.810-0.873 for **Ce(C3)$_2$(bipy)**, suggesting slightly more covalent Ce-C bonding for **Ce(C3)$_2$I** than **Ce(C3)$_2$(bipy)**. The Yb-C distances in **[Yb(C3)$_2$]I** range between 2.379(5)- 2.481(4) Å, and

the B-Yb-B angle is 155.3(1)°. The distortion from pseudo-octahedral geometry around the Yb(III) center is in contrast to that observed in the reported Tp* analogue, which has a crystallographically enforced B-Yb-B angle of 180°.

A similar and small amount of covalency in the Ln-C bonds was found for **Ce(C3)$_2$I** and **[Yb(C3)$_2$]I** using QTAIM analysis: $\frac{-G_{BCP}}{V_{BCP}}$ for the Yb-C bonds in **[Yb(C3)$_2$]I** (between 0.803 and 0.820) were similar to the values for **Ce(C3)$_2$I**, although in a narrower range, reflecting the narrower range of M-C distances in **[Yb(C3)$_2$]I** compared to **Ce(C3)$_2$I** (a result of greater symmetry).

It is instructive to compare the physical and electronic structures of **Ce(C3)$_2$(bipy)** with **Ce(Tp*)$_2$(bipy)**.[49] The SI contains an analysis of the steric similarity of **C3** and **Tp***.

Structurally, **Ce(C3)$_2$(bipy)** and **Ce(Tp*)$_2$(bipy)** are very similar, with B-Ce-B angles of 145.05(4) and 146.7(1)° respectively, while the Ce-N_{bipy} distances in **Ce(C3)$_2$(bipy)** are slightly longer than in **Ce(Tp*)$_2$(bipy)** (2.612(4) v.s. 2.592(4) Å) potentially due to more electron density on the cerium(III) center in **Ce(C3)$_2$(bipy)**, as a result of strong σ-donation from the tris(carbene) ligands.

The partial atomic charges for all the metal complexes were computed using the QTAIM and NPA schemes, Table S1 in the SI. As is normal, the metal atom charges are lower than their formal oxidation state of +3 in all cases due to ligand-to-metal electron (charge) transfer, which appears greatest for each **C3** adduct.

Analysis of $\boldsymbol{\rho_{BCP}}$ (electron density at BCP) and $\nabla^2\boldsymbol{\rho_{BCP}}$ (Laplacian of the electron density at BCP) suggest that the bonding for both the Ce-C bonds in **Ce(C3)$_2$(bipy)** and the Ce-N_{Tp*} bonds in **Ce(Tp*)$_2$(bipy)** are primarily ionic in nature. However, the slightly lower value of $\frac{-G_{BCP}}{V_{BCP}}$ at BCPs for the Ce-C bonds (0.810-0.873) in **Ce(C3)$_2$(bipy)** compared to the Ce- N_{Tp*} bonds in **Ce(Tp*)$_2$(bipy)** (0.874-0.921 Å), suggests slightly more covalent character for the Ce-C bonds in **Ce(C3)$_2$(bipy)**.

The calculations show that the frontier orbital energies for the Tp* complexes are slightly lower than those of their [**C3**] counterparts, for both the Ce bipy complexes and the Yb complexes (Figure 3 for Yb and Figure S5 for Ce in the SI). The SOMO-LUMO gaps for the bipy complexes are close in energy at 1.58 eV and 1.56 eV for **Ce(C3)$_2$(bipy)** and **Ce(Tp*)$_2$(bipy)**, while the SOMO LUMO gaps for **[Yb(C3)$_2$]I** and **[Yb(Tp*)$_2$]I** are 3.99 and 3.14 eV respectively (ignoring the electrons in the HOMO to HOMO-2 orbitals which are on the I^- counterion), suggesting greater oxidative stability for **[Yb(C3)$_2$]I**, in line with the observation that the attempts to prepare **Yb(C3)$_2$** instead generated **[Yb(C3)$_2$]I**, while **Yb(Tp*)$_2$** is reported to be isolable. Both bipy complexes exist in the triplet spin state with one electron on Ce and one on the bipy radical with unpaired electrons on the Ce center and the bipyridyl ligand. The UV-Vis absorption spectra of **Ce(C3)$_2$I** and **Ce(C3)$_2$bipy** were calculated using the time-dependent density functional theory (TD-DFT) method and were compared with the experimental spectra, with the computed spectra validating the theoretical predictions (Figures S1 and S3 in the SI, further details about these calculations and the frontier orbitals for the Ce complexes are also in the SI).

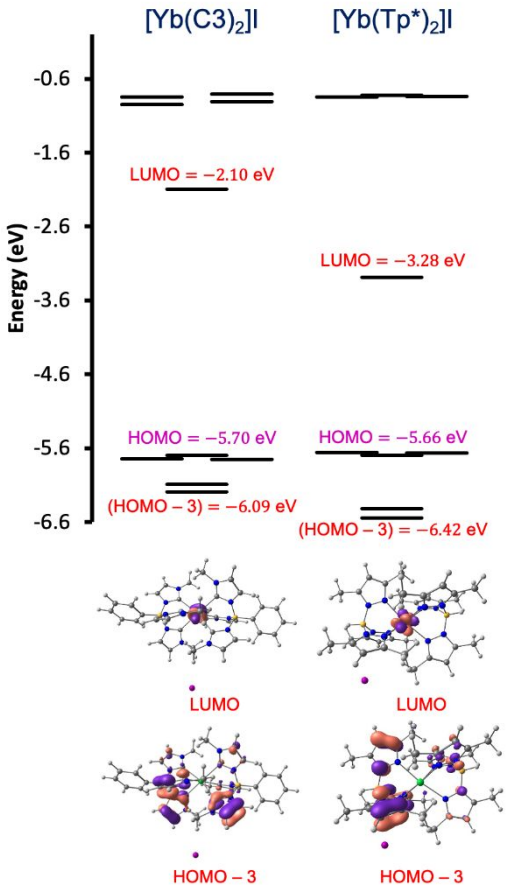

Figure 3. Calculated frontier molecular orbital diagrams for the Yb borate complexes. The three nearly degenerate HOMOs for the Yb complexes (shown in magenta) are exclusively localized on the non-bonded iodine ion.

The bonding is surprisingly different in the two Yb complexes: first, the LUMO in **[Yb(C3)$_2$]I** is f_{z^3} ($m_l = 0$, σ anti-bonding) while in **[Yb(Tp*)$_2$]I** it is computed to be f_{xyz} ($m_l = +2$, δ anti-bonding). Further, and in contrast with the Ce complexes, the unpaired spin in the 4f orbital of the Yb atom is confined within lower energy occupied molecular orbitals, rather than those near the HOMO. Comparing the two Yb complexes, the 4f orbitals of **[Yb(Tp*)$_2$]I** are more hybridized than those of **[Yb(C3)$_2$]I**, as indicated by the lower number of molecular orbitals with over 90% f-orbital contribution (only 3 in **[Yb(Tp*)$_2$]I** vs. 7 in **[Yb(C3)$_2$]I**). These data suggest the two different ligands can generate different preferred f-orbital use by the Ln center.

In conclusion, the coordination chemistry of tris(NHC) borates has been extended to the lanthanides cerium and ytterbium. Neutral molecular complexes of the form **Ln(C3)$_2$I** are favored for the larger cerium ion, while a separated ion pair of the form **[Ln(C3)$_2$]I** forms for ytterbium, resulting in dramatically different solubilities of the resulting complexes.

We suggest that this may have potential use in the separation of lanthanide ions. Calculated QTAIM metrics, including $\frac{-G_{BCP}}{V_{BCP}}$ suggest that the tris(carbene) borate ligands form slightly more covalent bonds with cerium and ytterbium than the N-donor tris(pyrazolyl)borates, and greater covalency calculated for the Ce-C bonds in **Ce(C3)$_2$I** than the bipyridyl adduct **Ce(C3)$_2$(bipy)**. Future work will study the use of these ligands to isolate specific rare earth ions and an investigation of their photophysical properties.

Conflicts of interest

The authors declare no conflicts of interest

Acknowledgements

The project was funded by the U.S. Department of Energy (DOE), Office of Science, Office of Basic Energy Sciences, Chemical Sciences, Geosciences, and Biosciences Division, in the Heavy Element Program (some synthetic efforts), the Molecular f-element qubits project (Yb complex analyses) and the Rare Earth Project in the Separations Program (remainder), at the Lawrence Berkeley National Laboratory under Contract DE-AC02-05CH11231. We acknowledge Hasan Celik for NMR support and the (NIH) for funding the NMR facility under grant nos. SRR023679A, S10OD024998 and 1S10RR016634-01.

References

1. R. A. Kresinski, in *Encyclopedia of Inorganic and Bioinorganic Chemistry*, 2012, DOI: 10.1002/9781119951438.eibc2032.
2. F. Mares, K. Hodgson and Streitwi.A, *J Organomet Chem*, 1970, **24**, C68-&.
3. F. Mares, K. O. Hodgson and Streitwi.A, *J Organomet Chem*, 1971, **28**, C24-&.
4. J. D. Jamerson, A. P. Masino and J. Takats, *Journal of Organomet Chem*, 1974, **65**, C33-C36.
5. J. Rausch, C. Apostolidis, O. Walter, V. Lorenz, C. G. Hrib, L. Hilfert, M. Kühling, S. Busse and F. T. Edelmann, *New Journal of Chemistry*, 2015, **39**, 7656-7666.
6. A. Greco, S. Cesca and W. Bertolini, *J Organomet Chem*, 1976, **113**, 321-330.
7. J. P. Durrant, B. M. Day, J. Tang, A. Mansikkamaki and R. A. Layfield, *Angew Chem Int Ed Engl*, 2022, **61**, e202200525.
8. N. Tsoureas, A. Mansikkamaki and R. A. Layfield, *Chem Commun (Camb)*, 2020, **56**, 944-947.
9. N. Tsoureas, A. Mansikkamaki and R. A. Layfield, *Chem Sci*, 2021, **12**, 2948-2954.
10. J. T. Boronski, L. R. Doyle, J. A. Seed, A. J. Wooles and S. T. Liddle, *Angew Chem Int Ed Engl*, 2020, **59**, 295-299.
11. J. T. Boronski and S. T. Liddle, *Eur J Inorg Chem*, 2020, **2020**, 2851-2861.
12. M. Xémard, S. Zimmer, M. Cordier, V. Goudy, L. Ricard, C. Clavaguéra and G. Nocton, *J. Am.Chem. Soc.,* 2018, **140**, 14433-14439.
13. L. Münzfeld, M. Dahlen, A. Hauser, N. Mahieu, S. K. Kuppusamy, J. Moutet, M. Tricoire, R. Köppe, L. La Droitte, O. Cador, B. Le Guennic, G. Nocton, E. Moreno-Pineda, M. Ruben and P. W. Roesky, *Angew. Chem. Int. Ed.*, 2023, DOI: 10.1002/ange.202218107.
14. R. A. Layfield, *Organometallics*, 2014, **33**, 1084-1099.
15. M. J. Heras Ojea, L. C. H. Maddock and R. A. Layfield, in *Organometallic Magnets*, Springer International Publishing, 2019, DOI: 10.1007/3418_2019_26, ch. Chapter 26, pp. 253-280.
16. P. Zhang, F. Benner, N. F. Chilton and S. Demir, *Chem*, 2022, **8**, 717-730.
17. P.-B. Jin, Y.-Q. Zhai, K.-X. Yu, R. E. P. Winpenny and Y.-Z. Zheng, *Angew. Chem. Int. Ed.*, 2020, **59**, 9350-9354.
18. E. Moreno-Pineda and W. Wernsdorfer, *Nature Reviews Physics*, 2021, **3**, 645-659.
19. K. Kundu, J. R. K. White, S. A. Moehring, J. M. Yu, J. W. Ziller, F. Furche, W. J. Evans and S. Hill, *Nat Chem*, 2022, **14**, 392-397.
20. M. Atzori, E. Garlatti, G. Allodi, S. Chicco, A. Chiesa, A. Albino, R. De Renzi, E. Salvadori, M. Chiesa, S. Carretta and L. Sorace, *Inorg. Chem.*, 2021, **60**, 11273-11286.
21. Y. Yao and Q. Shen, in *Rare Earth Coordination Chemistry*, 2010, DOI: 10.1002/9780470824870.ch8, pp. 309-353.
22. C. A. P. Goodwin, D. P. Mills in *The Lanthanides and Actinides*, ed. L. S. Natrajan, S. Liddle, D. P. Mills, World Scientific, 2022, DOI: 10.1142/9781800610163_0008, pp. 441-469.
23. P. L. Watson, T. H. Tulip and I. Williams, *Organometallics*, 2002, **9**, 1999-2009.
24. A. E. Kynman, L. K. Elghanayan, A. N. Desnoyer, Y. Yang, L. Severy, A. Di Giuseppe, T. D. Tilley, L. Maron and P. L. Arnold, *Chem Sci*, 2022, **13**, 14090-14100.
25. M. Poyatos, J. A. Mata and E. Peris, *Chem Rev*, 2009, **109**, 3677-3707.
26. P. L. Arnold and I. J. Casely, *Chem Rev*, 2009, **109**, 3599-3611.
27. M. Jalal, B. Hammouti, R. Touzani, A. Aouniti and I. Ozdemir, *Mater Today Proc*, 2020, **31**, S122-S129.
28. L. Zapf, U. Radius and M. Finze, *Angew Chem Int Ed Engl*, 2021, **60**, 17974-17980.
29. P. L. Arnold, M. S. Sanford and S. M. Pearson, *J Am Chem Soc*, 2009, **131**, 13912-13913.
30. I. S. Edworthy, A. J. Blake, C. Wilson and P. L. Arnold, *Organometallics*, 2007, **26**, 3684-3689.
31. M. E. Garner, S. Hohloch, L. Maron and J. Arnold, *Organometallics*, 2016, **35**, 2915-2922.
32. X. B. Carroll, D. Errulat, M. Murugesu and D. M. Jenkins, *Inorg Chem*, 2022, **61**, 1611-1619.
33. X. Gu, L. Zhang, X. Zhu, S. Wang, S. Zhou, Y. Wei, G. Zhang, X. Mu, Z. Huang, D. Hong and F. Zhang, *Organometallics*, 2015, **34**, 4553-4559.
34. X. Gu, X. Zhu, Y. Wei, S. Wang, S. Zhou, G. Zhang and X. Mu, *Organometallics*, 2014, **33**, 2372-2379.
35. J. F. DeJesus, R. W. F. Kerr, D. A. Penchoff, X. B. Carroll, C. C. Peterson, P. L. Arnold and D. M. Jenkins, *Chem Sci*, 2021, **12**, 7882-7887.
36. K. R. Meihaus, S. G. Minasian, W. W. Lukens, Jr., S. A. Kozimor, D. K. Shuh, T. Tyliszczak and J. R. Long, *J Am Chem Soc*, 2014, **136**, 6056-6068.
37. R. Fränkel, U. Kernbach, M. Bakola-Christianopoulou, U. Plaia, M. Suter, W. Ponikwar, H. Nöth, C. Moinet and W.

P. Fehlhammer, *J Organometallic Chem*, 2001, **617-618**, 530-545.
38. J. A. Valdez-Moreira, D. M. Beagan, H. Yang, J. Telser, B. M. Hoffman, M. Pink, V. Carta and J. M. Smith, *ACS Cent Sci*, 2021, **7**, 1751-1755.
39. T. Nishiura, A. Takabatake, M. Okutsu, J. Nakazawa and S. Hikichi, *Dalton Trans*, 2019, **48**, 2564-2568.
40. S. B. Munoz, 3rd, W. K. Foster, H. J. Lin, C. G. Margarit, D. A. Dickie and J. M. Smith, *Inorg Chem*, 2012, **51**, 12660-12668.
41. S. B. Muñoz, W. K. Foster, H.-J. Lin, C. G. Margarit, D. A. Dickie and J. M. Smith, *Inorg Chem* 2012, **51**, 12660-12668.
42. L. Wang, Z. Zhao, G. Zhan, H. Fang, H. Yang, T. Huang, Y. Zhang, N. Jiang, L. Duan, Z. Liu, Z. Bian, Z. Lu and C. Huang, *Light Sci Appl*, 2020, **9**, 157.
43. C. Apostolidis, A. Kovacs, A. Morgenstern, J. Rebizant and O. Walter, *Inorganics*, 2021, **9**, 44.
44. N. Marques, A. Sella and J. Takats, *Chem Rev*, 2002, **102**, 2137-2160.
45. R. E. Cowley, R. P. Bontchev, E. N. Duesler and J. M. Smith, *Inorg Chem*, 2006, **45**, 9771-9779.
46. I. Nieto, F. Cervantes-Lee and J. M. Smith, *Chem Commun*, 2005, DOI: 10.1039/b505985b, 3811.
47. A. P. Forshaw, R. P. Bontchev and J. M. Smith, *Inorg Chem*, 2007, **46**, 3792-3794.
48. R. Fränkel, C. Birg, U. Kernbach, T. Habereder, H. Nöth and W. P. Fehlhammer, *Angew Chem Int Ed*, 2001, **40**, 1907-1910.
49. F. Ortu, H. Zhu, M. E. Boulon and D. P. Mills, *Inorganics*, 2015, **3**, 534-553.
50. P. Fang, L. Wang, G. Zhan, W. Yan, P. Huo, A. Ying, Y. Zhang, Z. Zhao, G. Yu, Y. Huang, S. Gong, L. Duan, Z. Liu, Z. Bian and C. Huang, *ACS Applied Materials & Interfaces*, 2021, **13**, 45686-45695.
51. R. F. W. Bader, *Acc Chem Res*, 1985, **18**, 9-15.
52. V. E. J. Berryman, J. J. Shephard, T. Ochiai, A. N. Price, P. L. Arnold, S. Parsons and N. Kaltsoyannis, *Phys Chem Chem Phys*, 2020, **22**, 16804-16812.
53. V. E. J. Berryman, Z. J. Whalley, J. J. Shephard, T. Ochiai, A. N. Price, P. L. Arnold, S. Parsons and N. Kaltsoyannis, *Dalton Trans*, 2019, **48**, 2939-2947.
54. R. D. Shannon, *Acta Crystallographica A*, 1976, **32**, 751-767.
55. G. H. Maunder, A. Sella and D. A. Tocher, *Chem Commun*, 1994, DOI: DOI 10.1039/c39940000885, 885-886.